

# X-ray absorption spectroscopy at the Ni–K edge in *Stackhousia tryonii* Bailey hyperaccumulator

M. Ionescu,<sup>1\*</sup> N. P. Bhatia,<sup>1</sup> D. D. Cohen,<sup>1</sup> A. Kachenko,<sup>2</sup> R. Siegele,<sup>1</sup> M. A. Marcus,<sup>3</sup> S. Fakra<sup>3</sup> and G. Foran<sup>4</sup>

<sup>1</sup> Australian Nuclear Science and Technology Organisation, Sydney, Australia

<sup>2</sup> Faculty of Agriculture, Food and Natural Resources, The University of Sydney, Sydney, Australia

<sup>3</sup> Advanced Light Source, Lawrence Berkeley National Laboratory, California, USA

<sup>4</sup> Australian National Beamline Facility, Tsukuba, Japan

Received 8 October 2007; Revised 15 July 2008; Accepted 3 August 2008

Young plants of *Stackhousia tryonii* Bailey were exposed to 34 mM Ni kg<sup>-1</sup> in the form of NiSO<sub>4</sub>·6H<sub>2</sub>O solution and grown under controlled glasshouse conditions for a period of 20 days. Fresh leaf, stem and root samples were analysed *in vivo* by micro x-ray absorption spectroscopy (XAS) at the Ni–K edge. Both x-ray absorption near edge structure and extended x-ray absorption fine structure spectra were analysed, and the resulting spectra were compared with spectra obtained from nine biologically important Ni-containing model compounds. The results revealed that the majority of leaf, stem and root Ni in the hyperaccumulator was chelated by citrate. Our results also suggest that in leaves Ni is complexed by phosphate and histidine, and in stems and roots, phytate and histidine. The XAS results provide an important physiological insight into transport, detoxification and storage of Ni in *S. tryonii* plants. Copyright © 2008 John Wiley & Sons, Ltd.

## INTRODUCTION

*Stackhousia tryonii* Bailey (Stackhousiaceae) is an Australian rare perennial shrub, native of north-eastern Australia, and one of three reported Ni hyperaccumulating (>1000 mg Ni kg<sup>-1</sup> dry weight (DW) in any above-ground tissue) plants from the Australian continent.<sup>1</sup> This herbaceous plant has been reported to hyperaccumulate nickel in excess of 4% DW in leaf tissues, with no adverse effects on the plant physiology.<sup>2</sup> So far, over 320-Ni hyperaccumulators have been identified with the majority of these species located within tropical environments.<sup>3</sup> More recently, several additional examples of Ni hyperaccumulation have been found from the ultramafic soils in western and central regions of Turkey.<sup>4</sup>

Hyperaccumulation appears to be a genetic trait, as inferred by studies of hyperaccumulator and non-accumulator plants belonging to the same species.<sup>5</sup> Boyd and Martens<sup>6</sup> proposed five hypotheses that could potentially explain the evolutionary significance of the metal hyperaccumulating trait. These included (1) chemical defense against herbivores or pathogens; (2) drought resistance; (3) metal tolerance or disposal; (4) interference with neighbouring plants and (5) inadvertent uptake. The first explanation, termed the 'defense hypothesis' has been tested in great detail with the majority of studies demonstrating that the accumulated metal can account for the deterrent effect.<sup>7,8</sup> Studies investigating the remaining hypotheses are scarce and warrant further investigation.

The ability of *S. tryonii* to absorb, transport and store Ni in above-ground biomass has raised a number of questions currently being debated in the scientific literature. One such question is the chemical associations between Ni and ligands including oxygen, nitrogen or sulphur donors during uptake and translocation from the roots to leaves. Recently, it was suggested that malic acid was the dominant organic acid present in leaf extracts of *S. tryonii* following exposure to Ni; however, a precise physiological explanation was not determined.<sup>9</sup> In this way, Ni atoms may be chelated, and once fixed by these macro-molecules, may be prevented from further reacting and thus manifesting its known toxicity.

Here we employed *in situ* x-ray absorption spectroscopy (XAS) to further elucidate the presence of Ni-complexes in living tissues of *S. tryonii*. Synchrotron-based XAS has previously been used<sup>10–12</sup> to probe the coordination environment in several hyperaccumulator species as it requires minimal sample preparation, thus preserving the true elemental distribution within whole plant tissues without the need for abrasive pre-treatments.

In this report, we present results which suggest that Ni absorption and sequestration in various tissues of *S. tryonii* is achieved not by one unique Ni-complex, but by a combination of Ni-complexes, specific for roots, stems and leaves.

## EXPERIMENTAL

Young *S. tryonii* plants were collected from the tropical region of north-eastern Australia, as described elsewhere,<sup>13</sup> and grown in a controlled glasshouse environment. Plants were exposed to Ni concentration of 34 mM kg<sup>-1</sup>

\*Correspondence to: M. Ionescu, Australian Nuclear Science and Technology Organisation, Australia.  
E-mail: Mihail.Ionescu@ansto.gov.au

(as  $\text{NiSO}_4 \cdot 6\text{H}_2\text{O}_2$ ) applied as a solution and grown for a period of 20 days. Live plants were transported to beamline 10.3.2 at the Advanced Light Source, Berkeley, CA and examined using XAS.<sup>14</sup> Before irradiation, leaf, stem and root samples were severed from the plants and immediately placed on the Peltier cold stage, at a temperature *ca*  $-30^\circ\text{C}$ . X-ray absorption near edge structure (XANES) and extended x-ray absorption fine structure (EXAFS) spectra were collected in fluorescence mode on frozen tissues at the Ni– $\text{K}_\alpha$  absorption edge. Micro x-ray fluorescence ( $\mu$ -XRF) mapping was performed using a  $5\ \mu\text{m} \times 5\ \mu\text{m}$  beam, and XAS spectra were acquired using a  $16\ \mu\text{m} \times 7\ \mu\text{m}$  beam.

In addition, a set of aqueous Ni model compounds (10–100 mM) were prepared using analytical reagent grade salts obtained from Sigma-Aldrich. Salts included citrate ( $\text{HOC}(\text{COOH})(\text{CH}_2\text{COOH})_2$ ), phosphate ( $\text{H}_3\text{PO}_4$ ), phytate ( $\text{C}_6\text{H}_{18}\text{O}_{24}\text{P}_6$ ), chloride ( $\text{NiCl}_2 \cdot 6\text{H}_2\text{O}$ ), L-histidine ( $\text{C}_6\text{H}_9\text{N}_3\text{O}_2$ ), oxalate ( $\text{HOCCOOH}$ ), malate ( $\text{CH}_2(\text{COOH})_2$ ), sulphate ( $\text{NiSO}_4 \cdot 6\text{H}_2\text{O}_2$ ) and hydroxide ( $\text{Ni}(\text{OH})_2$ ). Ni–K edge XAS spectra were collected in fluorescence mode, using a broad x-ray beam,  $0.5\ \text{mm} \times 2.5\ \text{mm}$ . This experiment was

carried out at the Australian National Beamline Facility at the Photon Factory, Tsukuba, Japan.

All spectra from *S. tryonii* samples and Ni model compounds were analysed using the Athena and Artemis packages.<sup>15</sup>

## RESULTS AND DISCUSSION

$\mu$ -XRF imaging was used to determine Ni localisation *in planta*. Typical  $\mu$ -XRF maps obtained of stem, leaf and flower tissues are shown in Fig. 1(a)–(f)

The maps were colour coded, with the element of interest (Ni) in blue, and the most abundant element present (Ca) in red. In stem tissues, Ni was confined to the epidermal tissue and in bundles running parallel with the axis (Fig. 1(d)). These bundles correspond to the location of the vascular tissue.<sup>16</sup>

In leaf tissues, Ni concentration increased towards the tip of the leaf, a phenomenon previously observed in Ni hyperaccumulators. For example, Mesjasz-Przybyłowicz *et al.*<sup>17</sup> observed highest Ni concentration in the leaf margin

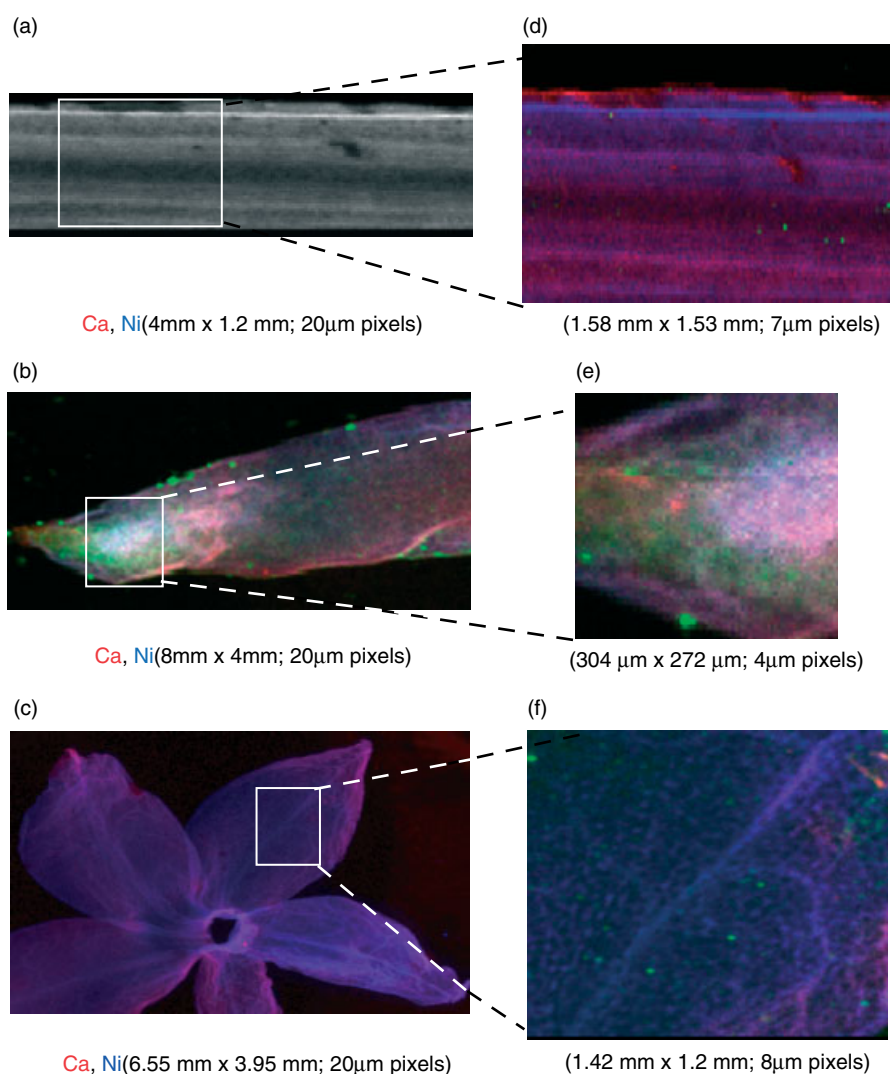


**Figure 1.** Typical coarse x-ray fluorescence maps of *S. tryonii* stem (a); leaf (b) and flower (c) at Ni–K absorption edge. Fine maps of stem (d); leaf (e) and flower (f) tissues depicted by a white box in (a)–(c) are also presented. The brighter areas represent higher concentrations of Ni (colour coded blue in the colour images). Spot size is indicated below each map.

( $22.1 \times 10^4 \text{ mg kg}^{-1} \text{ DW}$ ) of Ni-hyperaccumulating *Berkheya coddii* as compared to vascular bundles ( $1.58 \times 10^4 \text{ mg kg}^{-1} \text{ DW}$ ). Similarly, Severne<sup>18</sup> noted a maximum concentration of Ni in the leaf tip of Ni-hyperaccumulating *Hybanthus floribundus*. Most notable is the presence of Ni in the flower, which to our knowledge, has not been reported for this species.

Having employed  $\mu$ -XRF to determine the spatial localisation of Ni, we extracted normalised x-ray absorption spectra from selected regions (*hot spots*) of leaf, stem and root samples. The results of XAS spectra of *S. tryonii* leaf stem and root samples (Fig. 2) were reproducible, with the first scan being indistinguishable from the fourth or the fifth scan, suggesting that there was minimal, if any, radiation-induced change on the Ni environment in these samples.

The XANES spectra showed typical features associated with the valence and the coordination number of Ni-absorbing atoms, reported in literature.<sup>13,19</sup> The small pre-edge peak and the main absorbing peak revealed that Ni valence is  $2^+$ , and that the  $\text{Ni}^{2+}$  ion occupied an octahedral coordinated site. Since there is no energy shift in the position of these peaks as a function of the location of the absorbing Ni in any particular sample, or between different samples of leaf, stem or root, we conclude that there are no major changes in the Ni immediate atomic surrounding, as it is transported from the roots to the leaves. However, a close inspection of the absorption spectra in Fig. 2, showed a small decrease in the intensity of the main absorption peak (inset Fig. 2). This may be associated with a change in size or a distortion of the octahedral cage, which in turn may be caused by changes of all or some of the atoms surrounding the Ni.

In order to unravel the detailed information on the Ni environment contained in the fine structure of XAS spectra, we used the Artemis package. Various possible models of the Ni immediate atomic surrounding (first and second shells) were constructed, and the XAS spectra generated from these models were compared with the data obtained from the leaf, stem and root samples.

In spite of all efforts, we were unable to find a unique model that would reproduce the data in a satisfactory

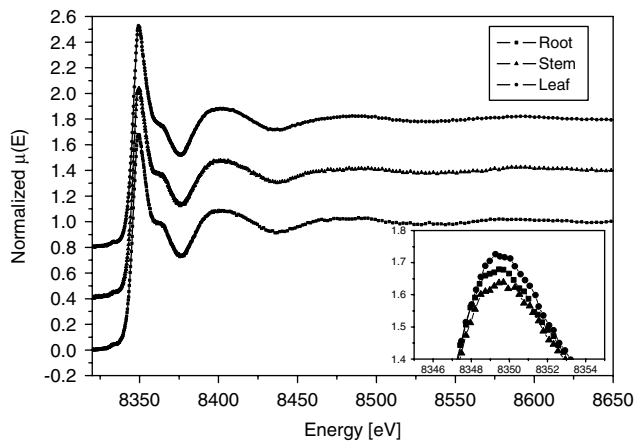


**Figure 2.** Normalised x-ray absorption spectra at Ni-K absorption edge from root (■), stem (▲) and leaf (●) tissues of *S. tryonii*.

way. A possible reason for this may be that there are multiple compounds that simultaneously chelate Ni in *S. tryonii*. In this case, the resulting XAS spectra collected from various parts of the plant would represent a superposition of all fluorescence signals from Ni and its surroundings contained in various chelators, and the construction of a structure model for these data would be impossible. Using this hypothesis, we considered a number of nine possible chelators for Ni. The selection criteria for these compounds were that (1) they had been identified in a Ni hyperaccumulator<sup>5,9-13</sup> or (2) they have been proposed on bio-physiology grounds as possible chelators of Ni in hyperaccumulators.<sup>2-4,6-8</sup>

The Ni-K edge XAS spectra of the Ni model compounds were also collected in fluorescence mode, but using a broad x-ray beam  $0.5 \text{ mm} \times 2.5 \text{ mm}$  (Fig. 3) and demonstrated that Ni was sensitive to the molecular environment of the  $\text{Ni}^{2+}$  central cation. As in the case of the plant samples, these spectra were also reproducible, with no noticeable change after repeated examination, suggesting that the immediate atomic surrounding of Ni was not modified under the influence of the beam.

Considering the possible hypothesis proposed above, we investigated if any linear combination of individual spectra from the nine Ni compounds could reproduce the fine structure of spectra collected from the plant samples (EXAFS). In the first instance, we limited the number of components to two, but the fitting results were unsatisfactory. Then we increased the number of components to three, which resulted in approximately 500 calculated spectra for each plant sample (leaf, stem and root).

All fitting calculations were carried out in *k*-space, and the results were sorted in order of the decreasing quality of the fit, given by the *R*-factor:

$$R = \frac{\sum(\text{experiment} - \text{fit})^2}{\sum(\text{experiment})^2} \quad (1)$$

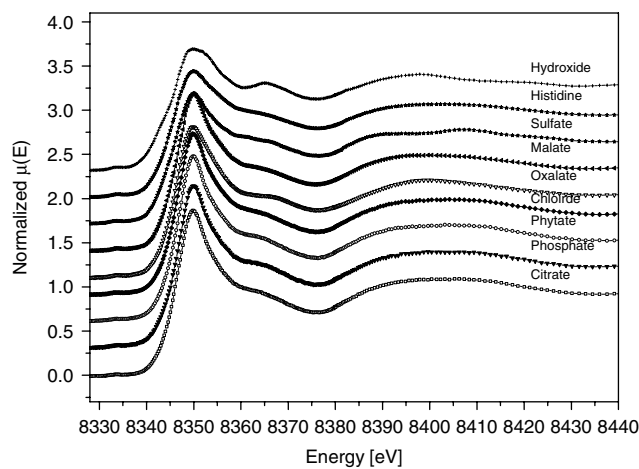


**Figure 3.** Normalised XAS spectra at Ni-K absorption edge from aqueous Ni compounds: citrate (□), phosphate (▼), phytate (◇), chloride (◆), oxalate (▽), malate (♣), sulphate (♠), histidine (\*), and hydroxide (+). Energy scale was limited to XANES, and all spectra less citrate were shifted up for clarity of display.

The lower the  $R$ -factor, the better the fit, and an  $R$ -factor  $< 0.02$  in general, reflect an acceptable fit. The best fit of the spectra using a linear combination of spectra from the nine model compounds provided pertinent information on the likely identity of the endogenous Ni ligands present in the tissues investigated.

The result of the best fit for leaf of *S. tryonii* ( $R$ -fit = 0.005) is given in Fig. 4, where (1) was obtained in energy, (2) in photoelectron wave vector ( $k$ ) space, and (3) the fit for the relative distance of scattering from absorber ( $R$ ) obtained by the Fourier transform of the  $k$ -space signal. In this lowest

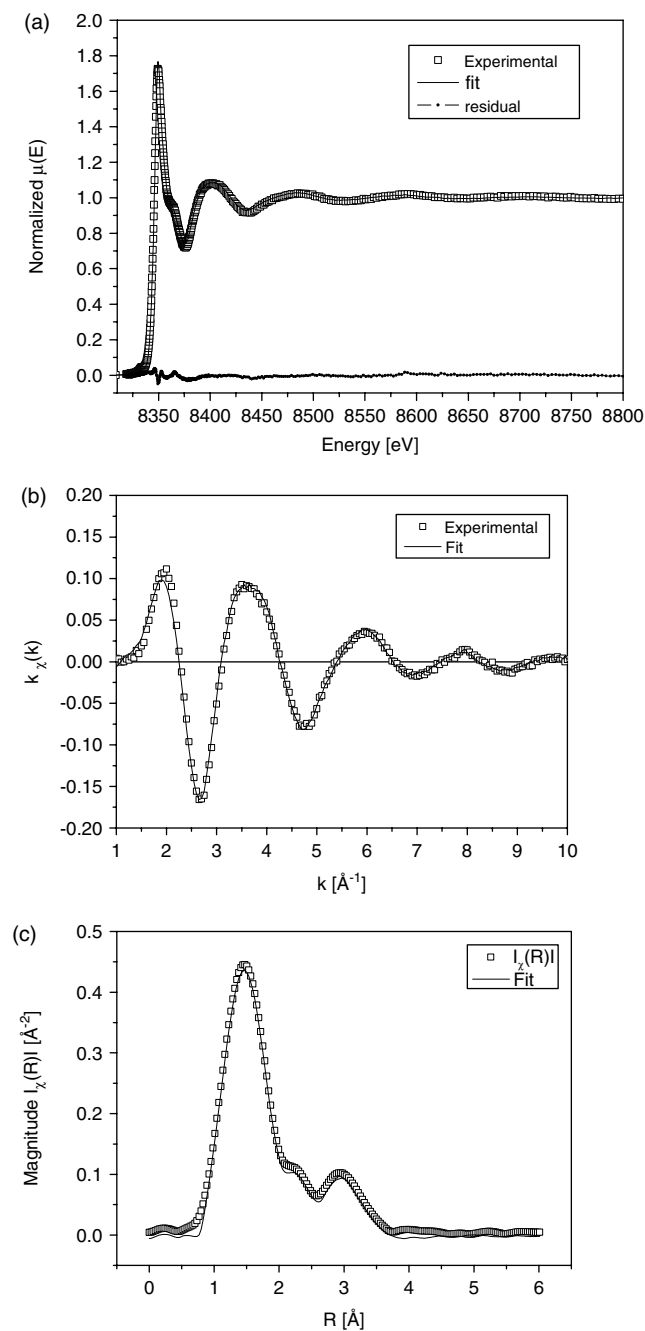


**Figure 4.** The fit result for normalised x-ray absorption spectra at Ni-K absorption edge from the leaf of *S. tryonii* for 61% citrate; 30% phosphate and 9% histidine; plotted against (1) energy; (2) wave vector  $k$  and (3) relative distance  $R$  of scatterer from the Ni absorber.

$R$ -fit case, the values of linear combination result are: citrate  $61 \pm 3\%$ , phosphate  $30 \pm 1.5\%$  and histidine  $9 \pm 0.5\%$ . This particular result suggested that Ni in leaves was found to be chelated by approximately 61% citrate, 30% phosphate and a small fraction of 9% by histidine.

Each fitting experimental result was given an 'experiment number' in order of increasing  $R$ -factor of the fit. In addition, for each experiment number, the result was displayed in the legend of each graph, as symbols of the various Ni-aqueous compounds, showing the contribution of each compound in percentage, as indicated by the linear combination fit. In this way, both the best fit (the lowest  $R$ -value), and the percentage of the three components of the linear combination can be visualised.

The results of the linear combination fit for the leaf sample of *S. tryonii* are shown in Fig. 5, where only the first 75 results are displayed. The results for stem and root samples are presented in Figs 6 and 7, respectively.

For leaves of *S. tryonii* the result presented in Fig. 5 suggests that the Ni present there was chelated by three

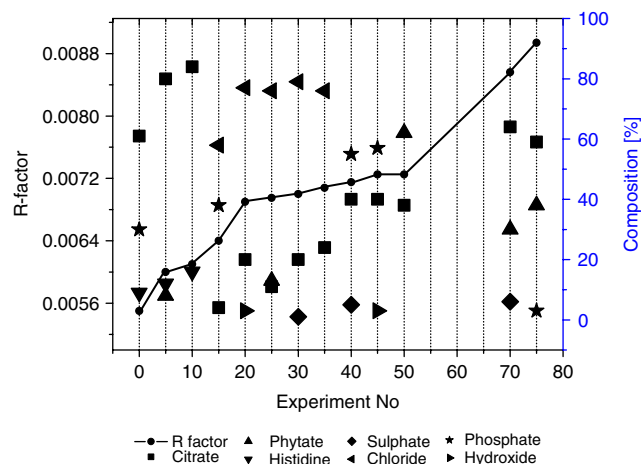


**Figure 5.** Leaf results of linear combination fit for *S. tryonii*, with the best-fit result for 61% citrate; 30% phosphate and 9% histidine.

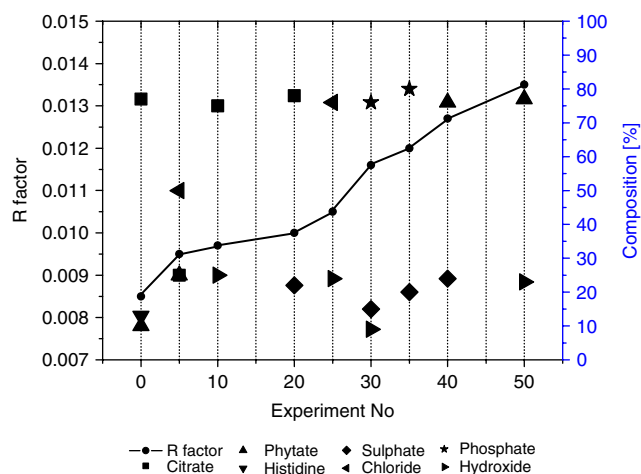


**Figure 6.** Stem results of linear combination fit for *S. tryonii*, with the best-fit result for 78% citrate; 10% phytate and 12% histidine.

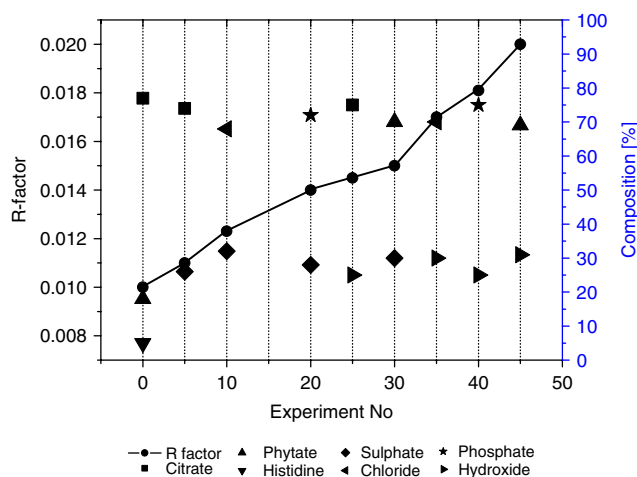


**Figure 7.** Root results of linear combination fit for *S. tryonii*, with the best-fit result for 77% citrate; 18% phytate and 5% histidine.

main compounds: citrate, phosphate and histidine. As seen in Fig. 5, citrate is the main component even for the higher values of *R*. This observation is also valid for stem (Fig. 6) and root (Fig. 7), strengthening the case that citrate may indeed be the main Ni–ligand.

These results are consistent to those of Krämer *et al.*<sup>5</sup> who employed XAS on leaves of Ni-hyperaccumulating *Thlaspi goesingense*.

These authors concluded that 87% of Ni not bound to the cell wall were chelated by citrate. Recently, Schaumlöffel *et al.*<sup>20</sup> investigated the Ni-hyperaccumulating *Sebertia acuminata* and indicated that 99.4% of the Ni in the water extract of latex (sap) was complexed by citrate. Similarly, Perrier *et al.*<sup>21</sup> employed EXAFS on leaves of *S. acuminata* that contained up to 2.5% Ni DW and suggested that Ni may be bound to citrate in the cell vacuoles.

The involvement of nitrogen–donor ligands, primarily free amino acids are assumed to play a role in hyperaccumulation; however, there remains much ambiguity as to their exact role. For example, Bhatia *et al.*<sup>13</sup> did not detect a significant increase in free amino acids in *S. tryonii* plants growing in low and high Ni soils and in the present study, histidine was the only amino acid observed when XAS data were fit. We report that 10% of Ni were chelated with histidine in leaf, stem and root tissues.

Krämer *et al.*<sup>22</sup> using high-performance liquid chromatography reported a 36-fold increase in the concentration of histidine in xylem sap of Ni-hyperaccumulating *Alyssum lesbiacum* after exposure to 0.3-mM Ni solution, as compared to control plants. A linear relationship between histidine and Ni has also been observed in Ni hyperaccumulating *Alyssum murale* and *Alyssum bertolonii* species and, moreover, EXAFS analysis has demonstrated that Ni is directly complexed with histidine in *A. lesbiacum*.<sup>22</sup>

More recently, the involvement of histidine in metal hyperaccumulation and possible detoxification has been questioned by others. For example, Persans *et al.*<sup>23</sup> using molecular and biochemical techniques, suggested that the histidine response was not a universal tolerance mechanism in Ni-hyperaccumulating species.

Authors investigated the histidine concentration in *T. goesingense* and *Thlaspi arvense* and reported no significant differences in histidine concentrations in xylem sap, roots and shoots during Ni exposure. Furthermore, the study found no changes in expression of three cDNA encoding enzymes involved in histidine biosynthesis. Indeed, Salt<sup>24</sup> agreed that histidine in *Thlaspi goesingense* was not involved in Ni hyperaccumulation and suggested other mechanism such as metal transport proteins may be involved.

## CONCLUSIONS

This study provides an insight into Ni localisation and complexation in fresh tissues of *S. tryonii*. Our results illustrate that the superposition of three compounds are responsible for chelating Ni in *S. tryonii*, and that the existence of a unique Ni-chelating compound is unlikely. We showed that it is possible that all XANES and EXAFS features of the absorption spectra obtained at the Ni–K absorption edge for leaves, stems and roots can be modelled with a linear combination of three separate known spectra. In the absence of a unique Ni-chelating compound, the small decrease in the intensity of the main absorption peak seen in the inset of Fig. 2, may be explained by the variation of the percentage fraction of the contributing spectra.

This study suggests that 61% of the Ni present in leaves are chelated by citrate, 30% by phosphate and 9% by histidine. Similarly, in stems and roots, 77% of Ni were associated with citrate. These results suggest that citrate may be involved in detoxification, transport and storage of Ni in *S. tryonii*.

## Acknowledgements

This work was partially supported by the Australian Synchrotron Research Program, which is funded by the Commonwealth of Australia under the Major National Research Facilities Program.

## REFERENCES

- Bhatia NP. Ecophysiology of nickel hyperaccumulation in *Stackhousia tryonii* Bailey. PhD Thesis, Central Queensland University, Australia, 2003.
- Batianoff GN, Specht RL. *The Ecology of Ultramafic (Serpentine) Soils*. Intercept Ltd: Andover, 1992; 109.
- Reeves RD. *Plant Soil* 2003; **249**: 57.
- Reeves RD, Adigüzel N. *Turkish J. Bot.* 2004; **28**: 147.
- Krämer U, Pickering IJ, Prince RC, Raskin I, Salt DE. *Plant Physiol.* 2000; **122**: 1343.
- Boyd RS, Martens SN. In *Proceedings of the First International Conference on Serpentine Ecology, University of California, Davis, USA*, Baker AJM, Proctor J, Reeves RD (eds). Intercept LTD: Andover, 1992; 279.
- Behmer ST, Lloyd CM, Raubenheimer D, Stewart-Clarke J, Kinght J, Leighton RS, Harper FA, Smith JAC. *Funct. Ecol.* 2005; **19**: 55.
- Boyd RS, Shaw JJ, Martens SN. *Am. J. Bot.* 1994; **81**: 294.
- Bhatia NP, Walsh KB, Baker AJM. *J. Exp. Bot.* 2005; **56**: 1343.
- Krämer U, Pickering IJ, Prince RC, Raskin I, Salt DE. *Plant Physiol.* 2000; **122**: 1343.
- Pickering IJ, Gumaelius L, Harris HH, Prince RC, Hirsch G, Banks JA, Salt D, George GN. *Environ. Sci. Technol.* 2006; **40**: 5010.
- Webb SM, Gaillard J-F, Ma LQ, Tu C. *Environ. Sci. Technol.* 2003; **37**: 754.

13. Bhatia NP, Backer AJM, Walsh KB, Midmore DJ. *Planta* 2005; **223**: 134.
14. Marcus MA, MacDowell AA, Celestre R, Manceau A, Miller T, Padmore HA, Sublett RE. *J. Synchrotron Radiat.* 2004; **11**: 239.
15. Ravel B, Newville M. *J. Synchrotron Radiat.* 2005; **12**: 537.
16. Bhatia NP, Walsh KB, Orlic I, Siegele R, Ashwath N, Baker AJM. *Funct. Plant Biol.* 2004; **31**: 1061.
17. Mesjasz-Przybyłowicz J, Przybyłowicz WJ, Pineda CA. *S. Afr. J. Sci.* 2001; **97**: 591.
18. Severne BC. *Nature* 1974; **248**: 807.
19. Bianconi A, Fritsch E, Calas G, Petiau J. *Phys. Rev., B* 1985; **32**: 4292.
20. Schaumlöffel D, Ouerdane L, Bouyssiere B, Lobinski R. *J. Anal. At. Spectrom.* 2003; **18**: 120.
21. Perrier N, Colin F, Jaffré T, Ambrosi J-P, Rose J, Bottero J-Y. *C. R. Geosci.* 2004; **336**: 567.
22. Krämer U, Cotter-Howells JD, Charnock JM, Baker AJM, Smith JAC. *Nature* 1996; **379**: 635.
23. Persans MW, Yan X, Patnoe J-MML, Krämer U, Salt DE. *Plant Physiol.* 1999; **121**: 1117.
24. Salt DE. *In Vitro Cell. Dev. Biol.-Plant* 2001; **37**: 326.